

Jan VRBKA, Miloš VLK and Vladimír KOTEK*

A Contribution to the Safety and Lifetime Assessment of Sintered Carbide WC-Co

* Faculty of Mechanical Engineering, Technical University of Brno,
Technická 2, 616 69 Brno, Czech Republic

Keywords: Strength conditions, lifetime, low cycle fatigue, biaxial testing device

ABSTRACT: *A proper modification of the Pisarenko's-Lebedyev's and combined Mohr's and maximum principal stress brittle fracture strength conditions was proposed for the safety evaluation, taking into account the plastic deformation in the compressive region. Two steps theoretical-experimental approach is suggested to estimate the low cycle fatigue. In the first one the stress time course is calculated at the most stressed construction element. In the second step, the lifetime is measured experimentally with the help of the testing machine for the cubic specimens under the 2-D cyclic loading.*

Introduction

Sintered carbide WC-Co belongs to the wide group of technical materials, exhibiting substantially different behaviour in tension and compression, see Fig.1

Because of much higher strength in compression than in tension the machine details are frequently prestressed in compression using for example overlaps in contact surfaces. A typical application is WC-Co matrix of the high pressure compound vessel (see Fig.2) used for production of superhard materials (synthetic diamond, cubic boron nitride etc.) and their sintering under pressure 5–8 GPa. The simplified time course of the internal pressure p_1 is illustrated at Fig.3. The first 6 points correspond to the deformation loading caused by overlaps Δr_j at contact surfaces (Fig.2) during the assembly process.

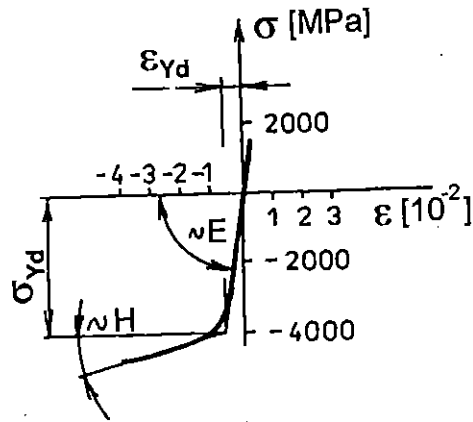


Fig. 1 Stress strain curve of sintered carbide WC-Co

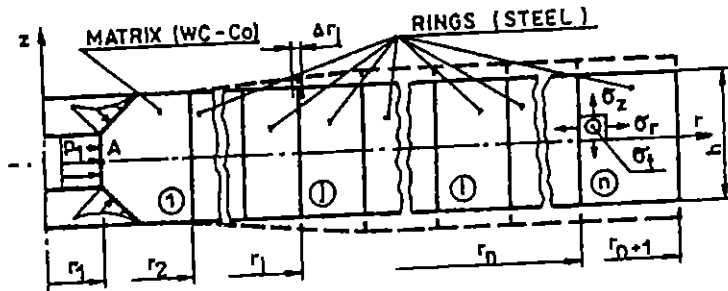


Fig. 2 High pressure compound vessel

Formulation of the strength condition

Application of the standard strength conditions used for brittle materials, such as Mohr's criterion, maximum principal stress or strain criterion and Pisarenko's - Lebedyev's criterion [1], [2] was not successful for the safety evaluation in the extreme compression region. For example the calculations by the finite element method (FEM) [3] made under presumption of linear elastic behaviour of sintered carbide WC-Co led to the calculated safety at the most stressed point A (Fig.2) $k_{RP} = 0.401$ for the compound vessel which was successful in service. The Pisarenko's - Lebedyev's condition was utilized for the safety

assessment. This value should be naturally higher than 1. To eliminate this discrepancy a specific calculation approach has been proposed, taking into account the plastic deformation in the compressive region, calculated with the help of associated plasticity theory, mixed hardening rule and modified Mises' plasticity criterion [3]. The plasticity function F is defined in effective stress space (Fig.4)

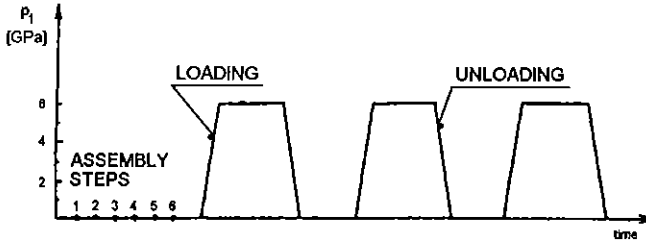


Fig. 3 Simplified time course of the loading.

$$F = \sigma_i \{ \sigma^* \} - \sigma_y^* (R, \varepsilon_i^{pl}, T) = 0 \quad (1)$$

where σ_i is stress intensity (3), $\{ \sigma^* \}$ is effective stress vector (2), σ_y^* is effective yield stress, R is Hill's coefficient of mixed hardening, ε_i^{pl} is plastic strain intensity and T is temperature.

$$\{ \sigma^* \} = \{ \sigma \} - \{ \alpha \} \quad (2)$$

$$\sigma_i = \sqrt{1.5 \{ s^* \}^T [M] \{ s^* \}} \quad (3)$$

Here $\{ \alpha \}$ denotes the position of the effective stress space (Fig.4), $\{ s^* \}$ is stress deviator vector and finally $[M]$ is transformation matrix [3]. In contrary to the 1-D stress state the definition of the compressive resp. tensile stress state is much more complicated under the 3-D stressing. A proper modification has been proposed to solve this problem. The plasticity surface Γ_y in Haigh's stress space is defined (Fig.4), according to the stress-strain curve in compression region (Fig.1). The actual stress states are restricted with the brittle fracture limiting surface Γ_R shifted together with the effective stress space if the mixed

hardening occurs. With respect to the real material characteristics the brittle fracture surface Γ_R in the tensile region is permanently inside the plasticity surface Γ_y and therefore no plastic deformation can arise here.

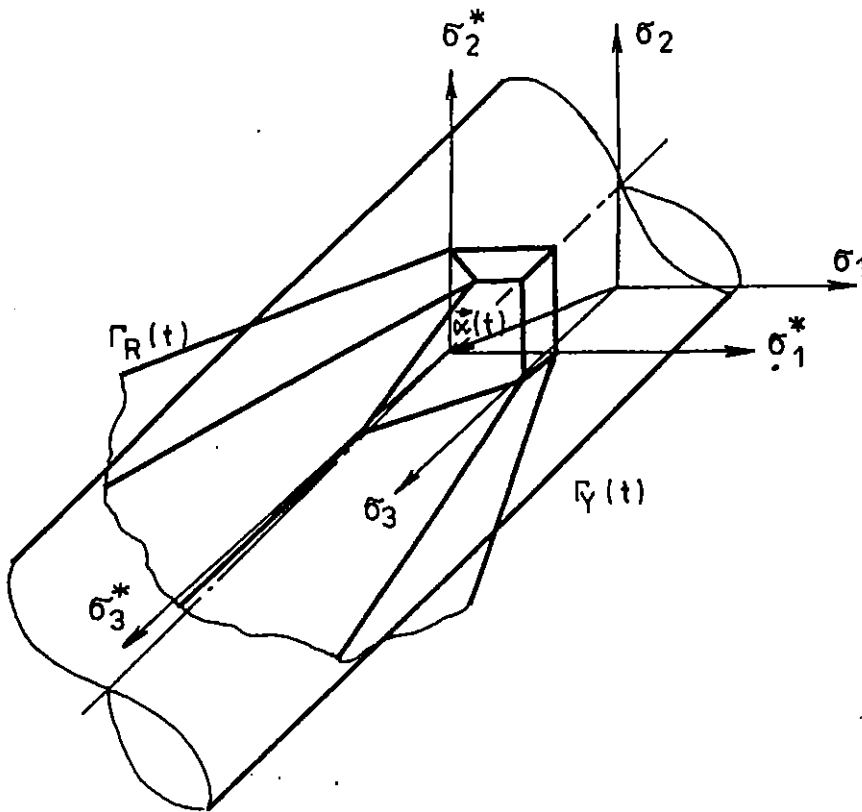


Fig. 4 Limiting surfaces of plasticity Γ_y and brittle fracture Γ_R in Haigh's stress space.

For each loading state the proportional safeties k_{RM} (corresponding to the combined Mohr's and maximum principal stress strength hypothesis) and k_{RP} (corresponding to the Pisarenko's-Lebedyev's strength hypothesis [1]) can be evaluated on the base of calculated principal stresses σ_1^* , σ_2^* and σ_3^* in effective stress space

$$k_{RM} = \frac{\sigma_{Rt}}{\max(\sigma_1^* - \kappa \cdot \sigma_3^*, \sigma_1^*)} \quad (4)$$

$$k_{RP} = \frac{\sigma_{Rt}}{\{\kappa \cdot \sigma_i^* + (1 - \kappa) \cdot \sigma_1^*\}} \quad (5)$$

Here σ_{Rt} describes the tensile strength, $\kappa = \sigma_{Rt} / \sigma_{Rd}$, where σ_{Rd} means the compressive strength. The problem oriented program system PROKOP [4] based on displacement version of finite element method (FEM) has been developed on these theoretical assumptions, which can simulate the whole loading history from the assembly beginning till the actual loading state (Fig.3) [3]. A loading parameter is defined to distinguish the loading and unloading part of the loading cycle. The non-linear mechanical problem is finally described with the help of FEM equilibrium equation in the incremental form

$$[K^{ep}] \cdot \{\delta\Delta\} = \{\delta f^p\} + \{\delta f^v\} + \{\delta f^d\} + \{\delta f^T\} = \{\delta f\} \quad (6)$$

where $[K^{ep}]$ means the global elastic-plastic stiffness matrix, $\{\delta\Delta\}$ is displacement incremental vector, $\{\delta f^p\}$, $\{\delta f^v\}$, $\{\delta f^d\}$ and $\{\delta f^T\}$ are generalised nodal forces increments caused by pressure, volume, deformation and temperature loading due to the nonhomogeneous temperature field. A method of controlled loading has been utilized for numerical solution of the non-linear elastic-plastic problem to simulate the cyclic loading most precisely.

Formulation of the low cycle fatigue condition

The formulation of the reliable enough low cycle fatigue conditions is more complicated problem. The searched general 3-D limit state condition should follow the known experimental data. The 1-D experimental investigations under the 1-D symmetrical cyclic loading have shown that after the short hardening period the saturation occurs with

the almost constant saturated strain amplitude $\epsilon_a^{p,s}$, see Fig.5. The loading stress amplitude σ_a during the tests was constant.

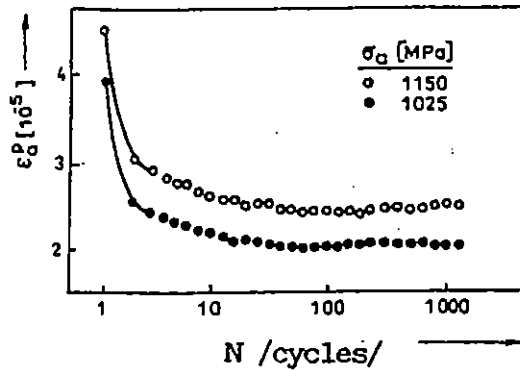


Fig. 5 Hardening curves for two stress amplitudes σ_a .

The characteristic hysteresis loop after saturation is presented at Fig.6

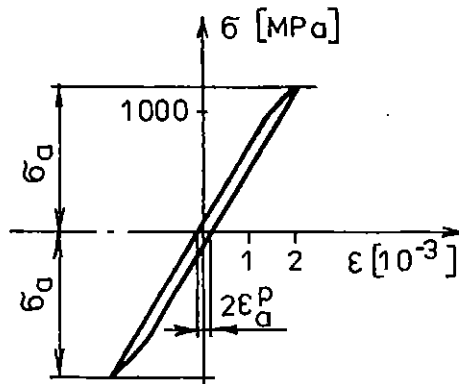


Fig. 6 Hysteresis loop after saturation.

On the basis of several experiments performed with different stress amplitudes, the Manson's-Coffin's relation between the saturated strain amplitude $\epsilon_a^{p,s}$ and lifetime N_f was obtained, see Fig.7.

The situation under the cyclic pulsating compressive loading exhibits somewhat different features. The cyclic stress-strain curve is illustrated at Fig.8. The existence of the cyclic creep under the applied high compressive cyclic loading is evident from the picture.

But even here the saturation occurs after appr. 10 loading cycles and the plastic strain amplitude $\epsilon_a^{p,s}$ does not change any more. Similar to the previous case the Manson's-Coffin's relation between the $\epsilon_a^{p,s}$ and the lifetime N_f can be obtained here.

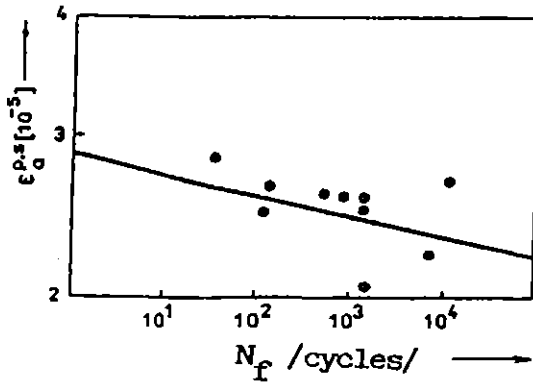


Fig. 7 Low fatigue lifetime curve for symmetric cyclic stress loading.

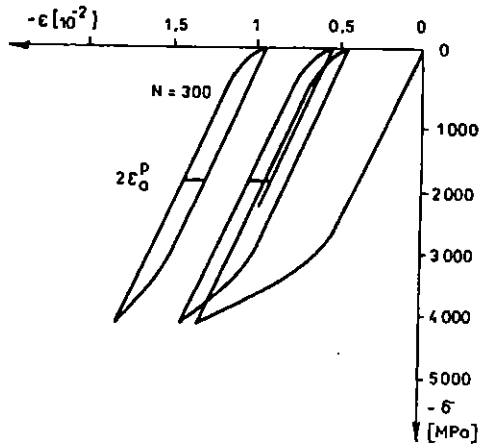


Fig. 8 Cyclic stress-strain curve for pulsating compressive loading.

In both cases we were restricted to the 1-D stress state. Now the idea arises if the Manson's-Coffin's curve in generalized form $\epsilon_{i,\sigma}^{p,s}$ related to the lifetime N_f could be applied in 3-D stress state. The parameter $\epsilon_{i,\sigma}^{p,s}$ means the amplitude of saturated plastic strain intensity. The dependence of the plastic strain intensity increments $\Delta\epsilon_i^p$ on the number of loading

cycles (Fig.3) in most stressed matrix element A (Fig.2) is presented at Fig.9. The kinematics hardening was assumed for the calculation performed with mentioned FEM code PROKOP [4]. It is evident from the picture, that the saturation phenomenon occurs even here.

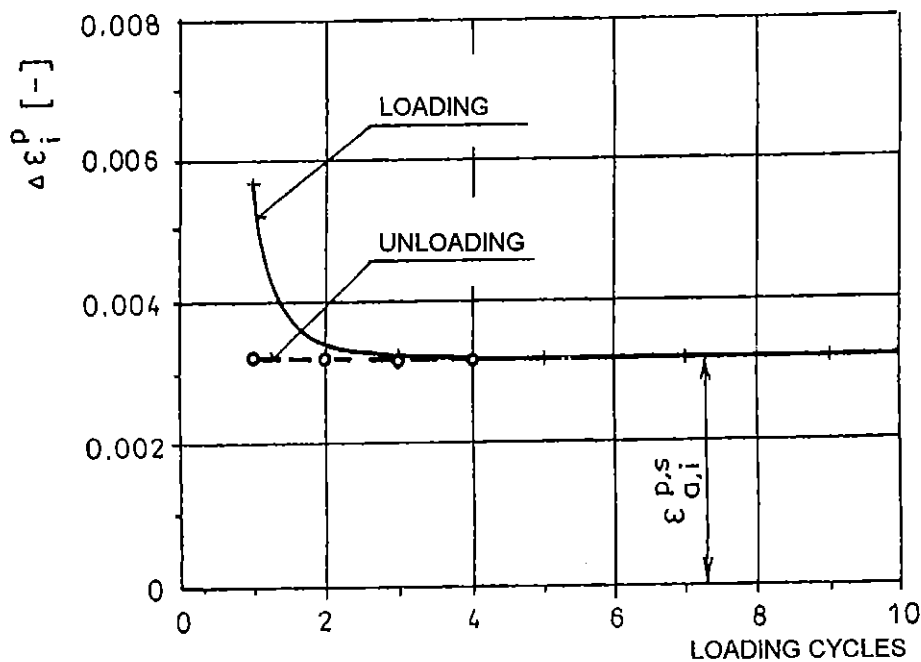


Fig. 9 Dependence of the plastic strain intensity increments $\Delta \epsilon_i^p$ on the number of loading cycles for kinematics hardening.

To assess the reliability of proposed method for the lifetime calculation on the basis of $\epsilon_{i,a}^{p,s}$ the comparison of values $\epsilon_{i,a}^{p,s}$ obtained for the same lifetime $N_f = 3000$ but under the different loading stress states has been done. In the case of 1-D symmetric cyclic loading the saturated value of plastic strain amplitude was $\epsilon_a^{p,s} = 2,5 \cdot 10^{-5}$ by the stress amplitude $\sigma_a = 1120 \text{ MPa}$. In the case of 1-D pulsating loading in compression the value was $\epsilon_a^{p,s} = 4,3 \cdot 10^{-4}$ by the low stress $\sigma_n = -4300 \text{ MPa}$ and finally in the calculated 3-D example (Fig.9) the saturated strain was $\epsilon_{i,a}^{p,s} = 3,2 \cdot 10^{-3}$ by the stress time course presented in Fig.10.

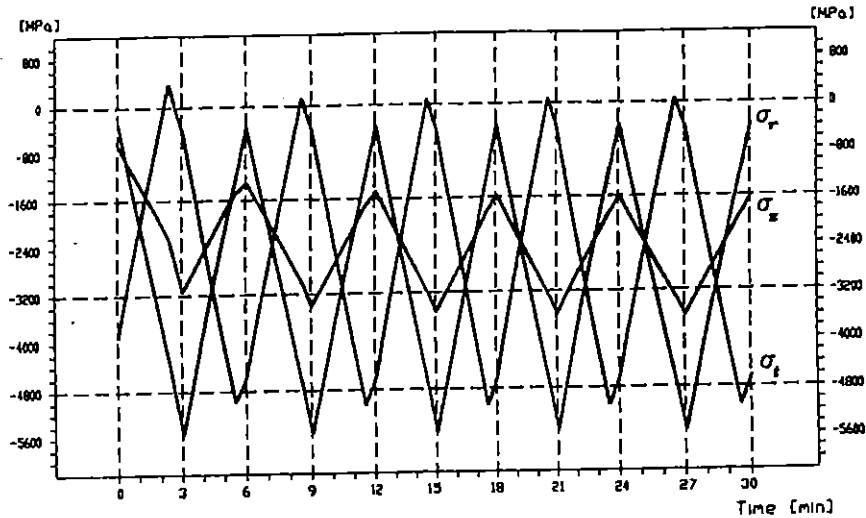


Fig. 10 Time course of radial, tangential and axial stresses σ_r , σ_t and σ_x in most loaded matrix element for kinematics hardening.

It is clearly evident from the analysis performed that for the lifetime assessment it is necessary to do an experiment with the similar stress state as in the critical element of the matrix. The combined theoretical-experimental approach was proposed to determine the lifetime of machine detail (matrix) made of sintered carbide WC-Co. In the first computational step, the stress time course in the most loaded machine part element (in our case point A at matrix - see Fig.2) is calculated, using FEM code PROKOP. In the second step the experiment is realized with cubic shape specimen made of WC-Co, with the loading corresponding to the calculated stress state in the most stressed construction element, see Fig.10. In investigated case the value σ_x can be neglected with respect to other two stresses and the assumption of the 2-D stress state can be accepted. A special experimental device was designed and manufactured for independent 2-D pressure loading of the cubic specimen (Fig.11) in the pressure range up to 5 GPa.

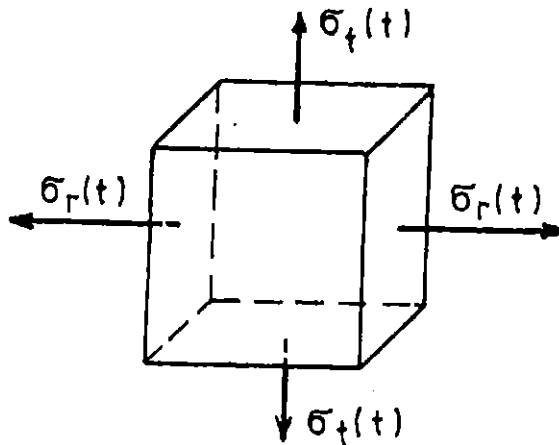


Fig. 11 2-D loading of the cubic element.

In the following picture (Fig.12) the loading part of the experimental device is illustrated. Because of the small displacements the pistonless simple construction with membranes could be utilized. Two independent pressure oil circuits were used to assure independent 2-D loading. Photos of the whole experimental device will be presented at the conference.

A corresponding attention was devoted to the tuning of the pressure oil circuit elements to obtain pressure time course approaching the harmonic or trapezoidal time course as much as possible. The deformation of the cubic element in two direction is measured with the help of two extensometers attached to the loading cones tips. The time course of the pressure loading as well as the deformation of the specimen in one direction is presented in Fig.13.

The cubic shape specimen is unusual in the experimental practice. To be able to judge the shape influence the comparison of compression strengths for cubic and traditional cylindrical specimens with diameter 5 mm and length 5 mm was performed under the static 1-D loading. The material was sintered carbide WC-Co G9 with Co content appr. 10% (producer PRAMET Šumperk). Two groups of 5 specimens were tested and average compressive strength and the standard deviation were calculated. The corresponding values were by the cubic specimens $\sigma_{Rd} = 3439 \pm 667\text{ MPa}$ and by the cylindrical specimens $\sigma_{Rd} = 3230 \pm 851\text{ MPa}$. It is clear, that the shape influence was not significant and the

cubic shape specimens can be accepted. In the case of such short specimens the random conditions at the contact surface between the specimen and loading cone tip are playing an important role.

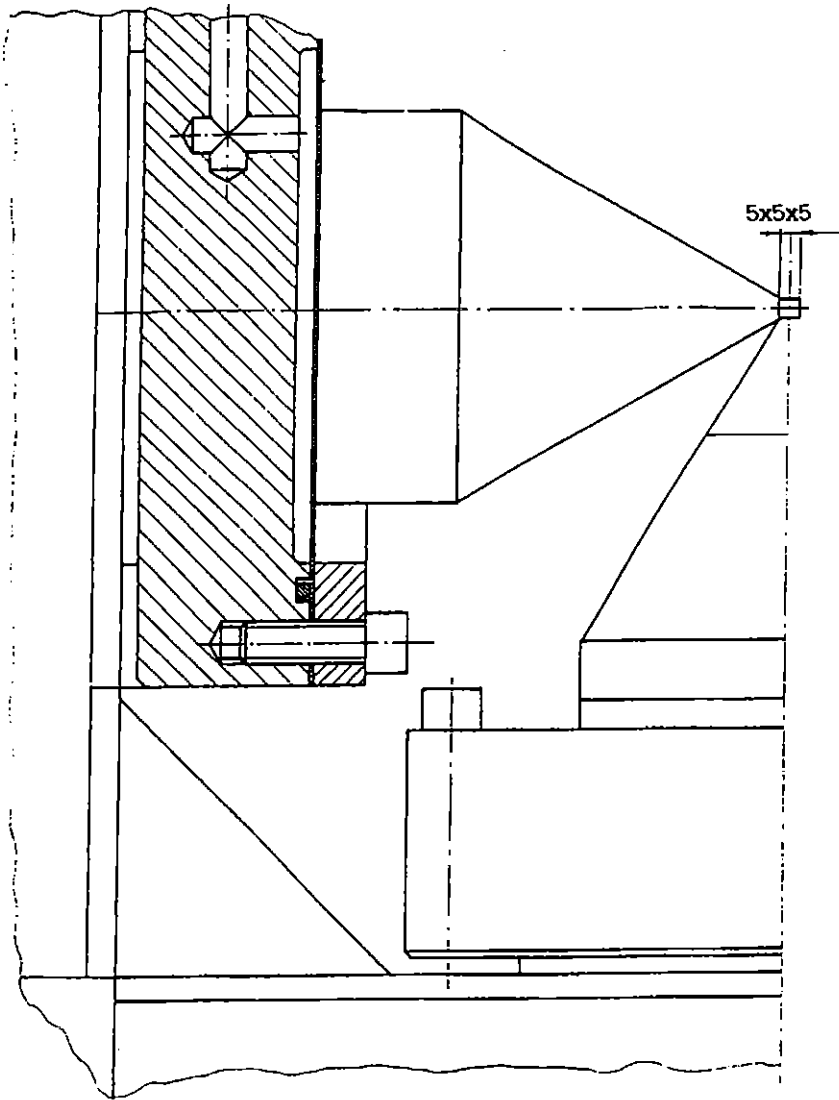


Fig. 12 Active loading part of the 2-D experimental device.

Results achieved

The stress analysis was done at the most stressed WC-Co matrix element A (Fig.2) by the compound vessel being successful in the service. The following material mechanical characteristics of WC-Co were used for FEM calculation [4] - elasticity modulus $E = 5,5 \cdot 10^5 \text{ MPa}$, hardening modulus $H = 5,2 \cdot 10^4 \text{ MPa}$, Poisson's ratio $\mu = 0,2$, model yield stress in compression $\sigma_{yd} = 4000 \text{ MPa}$ (Fig.1), yield stress corresponding to the first plastic deformation $\sigma_{yd} = 3000 \text{ MPa}$ (Fig.1), tensile strength $\sigma_{Rt} = 1200 \text{ MPa}$, $\mu = 0,28$. The stress analysis was performed for the first 10 loading cycles, see Fig.10. In accordance with hysteresis loop presented in Fig.7 the kinematics hardening rule was applied here. The calculated safeties increased from the unreal values $k_{RM} = 0,307$ and $k_{RP} = 0,401$ for the elastic material model to the more realistic $k_{RM} = 1,302$ and $k_{RP} = 1,485$ at the plastization beginning and to the $k_{RM} = 1,497$ and $k_{RP} = 1,904$ at the end of the loading part of the first loading cycle (Fig.3). Corresponding values at the end of the unloading part of the first loading cycle were $k_{RM} = 1,093$ and $k_{RP} = 1,233$. The safety values do not change substantially during the cyclic loading, for example at the of the loading part of the 10th loading cycle the safeties were $k_{RM} = 1,585$ and $k_{RP} = 1,979$ and at the end of the unloading part $k_{RM} = 1,052$ and $k_{RP} = 1,214$.

The proposed two steps theoretical-experimental approach was utilized to estimate the lifetime of WC-Co matrix. The calculated stress time course presented in Fig.10 was simplified in such a way, that the axial stress σ_z was neglected with respect to the tangential and radial stresses σ_t and σ_r , and the 2-D loading of the cubic specimen (Fig.11) was realized in the testing device (Fig.12). The results achieved will be presented at the conference.

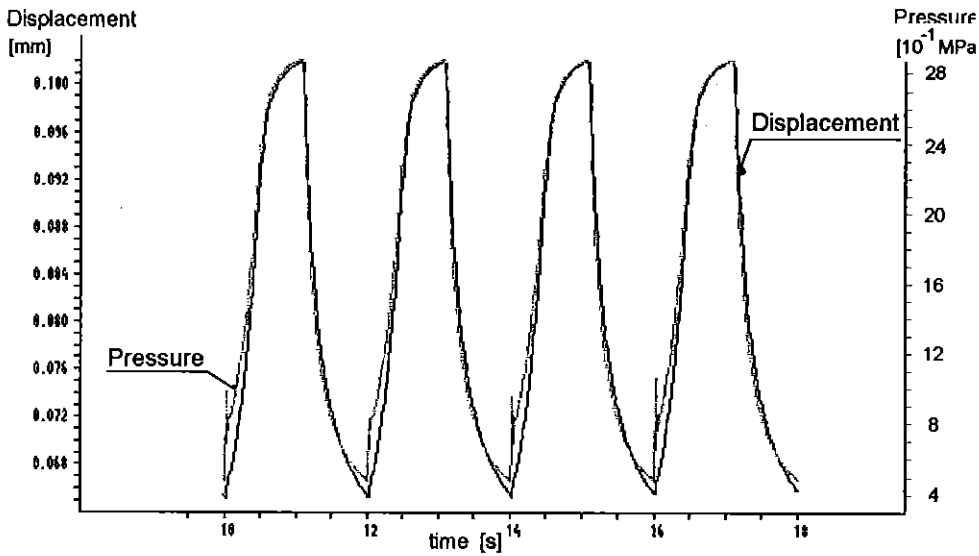


Fig. 13 The time course of the pressure loading and deformation of the specimen.

Conclusions

To be able to obtain the realistic safety coefficients by machine parts made of sintered carbide WC-Co loaded in compressive region, the plastic deformation has to be taken into account. The limiting fracture surface in Haigh's space is shifted together with the effective stress space, if mixed hardening occurs. The best results were achieved with the kinematics hardening rule and the Pisarenko's-Lebedyev's brittle fracture condition.

It is evident from the data presented in the paper, that the generalized Manson's-Coffin's approach based on the saturated plastic strain intensity $\varepsilon_{i,a}^{p,s}$ is not acceptable for the WC-Co lifetime predictions under the low cycle fatigue conditions. Two steps theoretical-experimental approach was proposed to estimate the lifetime and the special 2-D testing device for the cubic shape specimens was designed and manufactured.

References

- (1) PISARENKO G.S. and LEBEDJEV A.A., (1976), Deformation and strength of materials under the space stress state. Kiev, Naukova dumka, (in Russian)
- (2) GRIFFITHS T. et al, (1989) Use of stress analysis in design of PM structural components. Powder Metallurgy 32, pp.304-308
- (3) VRBKA J. and HOLUŠA L., (1993), FEM modelling of the elastic-plastic stress and strain of the axisymmetrical compound vessel with a component made of sintered carbide. Computers and Structures 48, pp.453-465
- (4) VRBKA J., HOLUŠA L. and VESELÝ V., (1993), RPS PROKOP/PC. Axisymmetric elasto-plastic problem. Reference manual. Technical University of Brno

Acknowledgment: This work was sponsored by the Czech Grant Agency under contracts numbers 101/94/0550 and 101/97/0836.